Journal of Power Sources 248 (2014) 642–646

Contents lists available at ScienceDirect

Journal of Power Sources

journal homepage: www.elsevier.com/locate/jpowsour

Short communication

Densification and ionic-conduction improvement of lithium garnet solid electrolytes by flowing oxygen sintering

Yiqiu Li [1], Zheng Wang [1], Chilin Li*, Yang Cao, Xiangxin Guo*

State Key Laboratory of High Performance Ceramics and Superfine Microstructure, Shanghai Institute of Ceramics, Chinese Academy of Sciences, 1295 Ding Xi Road, Shanghai 200050, China

HIGHLIGHTS

- Flowing oxygen sintering to improve lithium garnet electrolytes is firstly studied.
- Densification is enhanced by filling pores with oxygen and its lattice diffusion.
- A high density (96%) and overall conductivity (7.4×10^{-4} S cm^{-1}) are achievable.

GRAPHICAL ABSTRACT

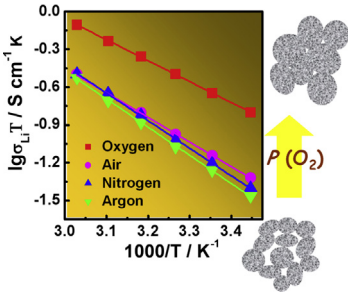

ARTICLE INFO

Article history:
Received 29 August 2013
Received in revised form
20 September 2013
Accepted 30 September 2013
Available online 9 October 2013

Keywords:
Lithium garnet electrolytes
Flowing oxygen sintering
Densification
Ionic conductivity

ABSTRACT

High density (~96%) garnet-type Al-contained $Li_{6.75}La_3Zr_{1.75}Ta_{0.25}O_{12}$ (LLZTO-Al) solid electrolytes are prepared by conventional solid-state reaction and the following flowing oxygen sintering process. An overall ionic conductivity as high as 7.4×10^{-4} S cm^{-1} at 25 °C is achievable, remarkably higher than that obtained by sintering in other atmospheres. The dependence of density and conductivity of solid electrolytes on sintering under different oxygen partial pressures is discussed. Atmosphere sintering is proved to be an effective method to improve the relative density of lithium oxide ceramics.

1. Introduction

Solid state electrolytes have attracted much attention owing to their potential application in all-solid-state lithium batteries, which are thought to be superior to the presently used liquid-electrolyte based ones in terms of safety and environmental issues [1,2]. So far, a large number of solid state electrolyte prototypes have been reported, such as amorphous nitrided phosphate (LiPON) [3,4], perovskite-type titanates [5], NASICON-type phosphates [6], LISICON-type sulfides [7], and their glass–ceramic analogs [8,9]. Recently, the cubic $Li_7La_3Zr_2O_{12}$ (LLZO), a typical garnet framework oxide, showed a high ionic conductivity of approximately 2×10^{-4} S cm^{-1} at room temperature, as well as good thermal and chemical stabilities [10–12]. Stabilization of cubic garnet LLZO may need introduction of e.g. Al, Nb or Ta [13–15], since formation of tetragonal LLZO is also possible while causing a poor ionic conductivity [16]. Besides the crystalline structure, the microstructure related to grains and grain boundaries is also a critical issue. For

* Corresponding authors. Tel.: +86 21 52411030, +86 21 52411032; fax: +86 21 52411802.
E-mail addresses: chilinli@mail.sic.ac.cn (C. Li), XXGuo@mail.sic.ac.cn (X. Guo).
[1] The authors have the equal contribution to this work.

0378-7753/$ – see front matter © 2013 Elsevier B.V. All rights reserved.
http://dx.doi.org/10.1016/j.jpowsour.2013.09.140

polycrystalline ceramic electrolytes, a dense material with large grain size is highly desired. High porosity in solid electrolytes may cause a high grain boundary resistance as well as mechanical failure. Owing to the volatilization of Li components or inert gas filling in pores during sintering, the LLZO solid electrolytes obtained via conventional solid state method usually show a limited density as well as ionic conductivity. High density LLZO can be obtained by hot-pressing, which enables a relative density of 96–98% [16–18]. However, this technique is unsuitable for continuous mass production, and its production cost is high.

Flowing oxygen sintering is a powerful and economical alternative method, which had been used to prepare high density Pb-based piezoelectric ceramics [19–21]. Flowing oxygen during sintering can facilitate sintering by filling pores with pure oxygen, aiding densification compared with other molecules in air or inert atmospheres. To the best of our knowledge, this technique has not been applied in garnet-type solid electrolytes. In view of the good solubility and diffusivity of oxygen, the pores filled with oxygen could disappear easily by oxygen migration via lattice diffusion or vacancy transport. Therefore, we expect that the pure oxygen sintering can significantly enhance both the density and ionic conductivity of solid electrolytes. In this work, we compare the Al-contained $Li_{6.75}La_3Zr_{1.75}Ta_{0.25}O_{12}$ (LLZTO-Al) solid electrolytes which undergo the sintering processes with different oxygen partial pressures, respectively using oxygen, air, nitrogen and argon atmospheres. Their relative densities, microstructures and ionic conductivities are discussed, highlighting oxygen-sintering driven densification mechanism and conduction performance.

2. Experimental

LLZTO-Al ceramics were prepared via conventional solid state reaction, from stoichiometric LiOH (Alfa Aesar, 99.995%), $La(OH)_3$ (Alfa Aesar, 99.95%), ZrO_2 (Aladdin Reagent, 99.99%), Ta_2O_5 (Aladdin Reagent, 99.99%) and a 15 wt.% excess of LiOH for compensating volatile Li components during synthesis. The powders were ball-milled for 12 h, and then were heated in air at 900 °C for 12 h to ensure the formation of cubic LLZTO phase, and then were ball-milled for 12 h again. After that, the powders were pressed into pellets with a diameter of 12 mm at 100 MPa, and sintered at 1140 °C for 9 h in different atmospheres, i.e. oxygen, air, nitrogen and argon, respectively. During sintering the pellets were covered with their respective mother powders and put in covered alumina crucibles in a tube furnace.

The relative density values were obtained by the Archimedes method using alcohol (C_2H_5OH) for measurement. Crystalline structure of synthesized phases was obtained by X-ray diffraction (XRD, Bruker D2 Phaser), using Cu $K\alpha$ radiation with 2θ in range of 10–80° and step size of 0.02° and was rechecked at the beamline of BL14B1 in the Shanghai Synchrotron Radiation Facility. Their lattice parameters were estimated from Rietveld refinement by using Fullprof software. The compositions of LLZTO-Al samples were determined by inductively coupled plasma optical emission spectroscopy (ICP-OES, Agilent 725). Microstructure and morphology were characterized by scanning electron microscope (SEM, Hitachi S-3400N) at a 5 kV accelerating voltage, as well as transmission electron microscope (TEM, JEOL JEM-2100F) at a 200 kV accelerating voltage. Elemental distribution in grains and grain boundaries was detected by energy dispersive X-ray detector (EDX, IXRF Model 550i) equipped on SEM. Two sides of the pellet samples were polished and coated with dry Au slurry films with a diameter of 8 mm for the measurements of alternating current impedance and directing current polarization. Ionic conductivities of LLZTO-Al samples were measured in air in a temperature range from 20 to 60 °C, and in a frequency range from 0.1 Hz to 20 MHz with an amplitude of 10 mV using an impedance analyzer (Novocontrol Beta High Performance Impedance Analyzer). Electronic conductivities were examined by potentiostatic polarization experiment, using a battery test station (Arbin BT-2000) with an applied voltage of 5 V.

3. Results and discussion

The preparation of LLZTO-Al ceramics is characterized by different atmosphere sintering. The element composition of samples determined by ICP-OES is listed in Table 1. The mole ratios of La/Zr/Ta in these samples are almost the same, very close to the expected composition as shown in stoichiometric $Li_{6.75}La_3Zr_{1.75}Ta_{0.25}O_{12}$, e.g. Li:La:Zr:Ta:Al = 7.40:3:1.75:0.26:0.23 for oxygen-sintered sample. Note that all the samples show a bit higher lithium content than expected (e.g. 7.4 mol of Li exceeds 6.29 mol of Li required for charge balance in oxygen-sintered sample), which likely stems from Al reaction with Li to precipitate Li–Al–O phases at grain boundaries as discussed later [22]. Indeed, a certain amount of Al (~24 mol%) was detected from ICP-OES. It should come from the Al_2O_3 crucibles used for sintering, since no Al is intentionally added in the starting materials. Fortunately, Al contamination has been indicated to be beneficial to the improvement of conductivity, serving as grain boundary additive and/or lattice dopant [13,14,22]. The relative densities of the samples sintered in oxygen, air, nitrogen and argon are approximately 96%, 93%, 91% and 90%, respectively, through measuring three samples for each atmosphere by Archimedes method. It indicates that pure oxygen atmosphere can significantly increase the LLZTO-Al density, which is comparable to the value obtained by hot-press sintering [16,17].

Fig. 1 shows the X-ray diffraction (XRD) patterns for LLZTO-Al samples sintered in different atmospheres. Each of them displays a typical cubic garnet phase similar to $Li_5La_2Nb_2O_{12}$ (JCPDS 01-084-1753), and no obvious impurity phases can be detected. The lattice parameters from Rietveld refinement are ~12.96 Å for all the samples, close to the values reported in other Ta-doped LLZO with the same Ta content [17]. This result indicates that the three dimensional garnet framework is quite stable even in inert atmosphere sintering [23], and no serious oxygen evolution and structure collapse occur compared with less stable oxides of layer structures at high temperature.

In contrast to other atmospheres, sintering in pure oxygen leads to a much denser microstructure from the scanning electron microscope (SEM) images of cross sections of LLZTO-Al samples as shown in Fig. 2(a–d). Its grain size mainly lies in the range from 5 to

Table 1
Composition, relative density, lattice parameter a, total conductivity (σ_{total}), activation energy for total conductivity (E_a) and electronic conductivity (σ_e) of LLZTO-Al electrolytes depending on sintering atmospheres (oxygen, air, nitrogen and argon).

Sintering atmosphere	Atomic ratio of Li:La:Zr:Ta:Al[a]	Relative density (%)	Lattice parameter a (Å)	σ_{total} (S cm^{-1})	E_a (eV)	σ_e (S cm^{-1})
Oxygen	7.40:3:1.75:0.26:0.23	96	12.964	7.4×10^{-4}	0.33	2.1×10^{-7}
Air	7.53:3:1.75:0.26:0.24	93	12.963	2.4×10^{-4}	0.39	1.2×10^{-7}
Nitrogen	7.48:3:1.76:0.26:0.25	91	12.963	2.1×10^{-4}	0.43	9.0×10^{-8}
Argon	7.57:3:1.75:0.25:0.25	90	12.962	1.8×10^{-4}	0.44	6.2×10^{-8}

[a] Atomic ratio of Li:La:Zr:Ta:Al is normalized by La content as shown in the formula $Li_{6.75}La_3Zr_{1.75}Ta_{0.25}O_{12}$.

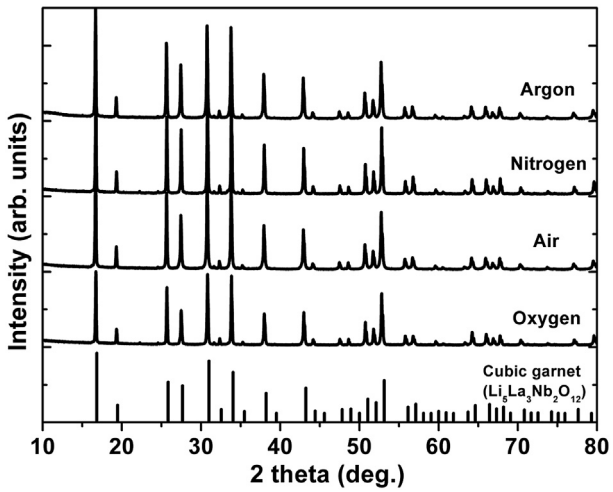

Fig. 1. XRD patterns for LLZTO-Al sintered in oxygen, air, nitrogen and argon atmospheres respectively. The diffraction patterns of cubic garnet $Li_5La_3Nb_2O_{12}$ (JCPDS 01-084-1753) are labeled as a reference.

10 μm, and the grain boundaries are reduced owing to grain growth and mergence. In other atmospheres, the grains are much smaller with size ranging mainly from 1 to 5 μm. Nonuniform pores are clearly observed due to incomplete intergranular contact. Note that the grain size in air is overall the same with those in inert atmospheres. It is possible that a high fraction of nitrogen in air (78%) seriously counteracts the oxygen effort on grain growth. Thus, one can conclude that flowing oxygen sintering can remarkably promote the grain growth and expel the pores from grain boundaries, leading to density enhancement of LLZTO-Al.

Composition analysis on grains and grain boundaries was carried out using energy dispersive X-ray detecting (EDX) technique (Fig. 2e). For all the samples, the Al element is mainly detected at grain boundaries rather than within intragrain zones, although we cannot rule out a tiny amount of Al is doped into the cubic phase of LLZTO-Al. Actually, the true role of Al^{3+} on either substituting Li sites or helping sinter is still on debate [15]. Considering that no Al-contained crystalline phase is detected by XRD, it is indicated that the grain boundaries consist of Al-contained glassy phases, likely Li–Al–O from the excess Li content by ICP. It is also in accordance with the color contrast in TEM image of Fig. 2f, which shows glass-like phase between two grains. No other crystalline phase is discernable apart from garnet-type diffractogram in the selected-area electron diffraction (SAED) pattern. The location of amorphous Li–Al–O phases at grain boundaries is likely another potential factor contributing to densification of LLZTO-Al apart from atmosphere sintering. We assume the same effect of Al in all atmospheres, since at least Al content is the same in all samples. It is predicted that Al-doped LLZO has a slightly larger lattice parameter ~13.03 Å for 23 mol% Al doping [24]. Therefore, it is possible that

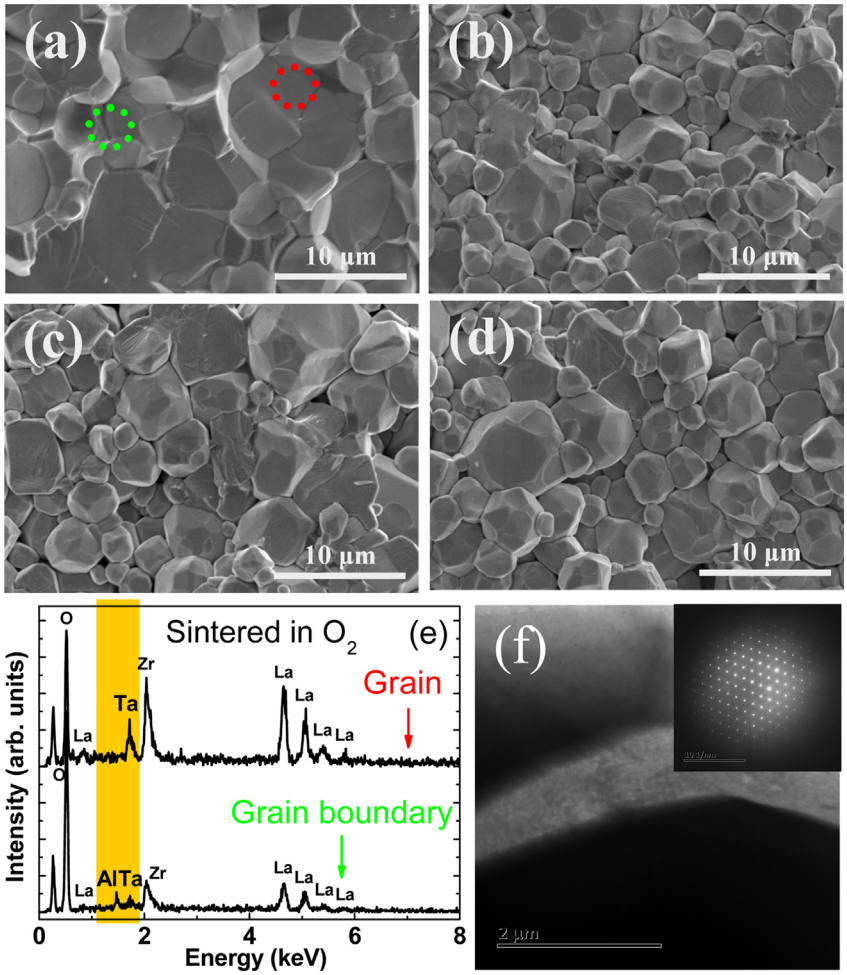

Fig. 2. Cross-section SEM images of LLZTO-Al electrolytes sintered in different atmospheres: (a) oxygen, (b) air, (c) nitrogen, (d) argon. (e) EDX element distribution on intragrain and grain boundary zones shown in red and green circles in (a). (f) TEM image of grain boundary zone, inset of (c): diffractogram of a typical garnet structure. (For interpretation of the references to colour in this figure legend, the reader is referred to the web version of this article.)

when Ta is present in the lattice it may prevent Al from entering compared to the case free of Ta. This also suggests that most of the Al reacts with Li to form Li–Al–O at grain boundaries. Removing Li–Al–O phase by selective etching is expected to be an effective method to further confirm the role of Li–Al–O phase, e.g. as Li-ion transfer promoter at grain boundaries, by comparing the conductivity difference with untreated sample.

The Nyquist plots of LLZTO-Al samples measured at 25 °C are shown in Fig. 3a. All the plots show a semicircle at high-medium frequencies, which is connected with a remarkable diffusion tail at low frequencies. The semicircle is associated with the total resistance (R_{total}) with a capacitance falling into the order of 10^{-9} F, indicating that the contribution of grain boundaries is involved [25]. However it is difficult to accurately separate grain boundary from lattice by modeling the impedance. The diffusion response at low frequencies is caused by the ion-blocking electrode which usually is Au. As shown in Table 1, the total conductivities (σ_{total}) are calculated according to $\sigma_{total} = L(SR_{total})^{-1}$, where L and S are the sample thickness and electrode area respectively. The oxygen sintered samples show the highest σ_{total} of 7.4×10^{-4} S cm^{-1}, which is at least 3 times larger than those under sintering in inert-gas contained atmospheres. Since the lattice conductivity is most likely the same for all samples, the difference in total conductivity is mainly due to the microstructural porosity and thus the contribution of resistive grain boundaries. Potentiostatic polarization behavior of LLZTO-Al samples was carried out to check their electron conduction contribution (Fig. 2b), which can be estimated from the steady state current of current–time profile [26], and is found to be at least 3 orders of magnitude lower than the ionic one for all the samples (Table 1), demonstrating the dominant Li-ion conduction of LLZTO-Al materials. However, so far it is unclear why electronic conductivity decreases with lower oxygen content gases (e.g. argon) vs high oxygen content gas (oxygen).

From the Arrhenius plots of total conductivities (σ_{total}) in Fig. 4, we can estimate the activation energy (E_a) according to $\sigma_{total}T = A\exp[-E_a(k_BT)^{-1}]$, where A is the pre-exponential parameter, k_B the Boltzmann constant and T the absolute temperature. As expected, the oxygen sintered samples show a lowest E_a of 0.33 eV, while the E_a values for samples sintered in inert-gas contained atmospheres range from 0.39 to 0.44 eV. The reduced activation energy further indicates the less involved grain boundary contribution, which usually decreases ion mobility or depletes ion concentration compared with the intragrain contribution. It has been reported that the hot-pressed $Li_{7-x}La_3Zr_{2-x}Ta_xO_{12}$ ($x = 0.25$) showed a lower activation energy 0.22 eV for the total conductivity [17], although with similar composition, density and conductivity as our oxygen sintered samples. These results suggest the importance of microstructure on Li-ion conduction behavior in solid electrolytes, despite they may share the same conduction mechanism in lattice structure. In hot-pressing applied stress might help oxygen diffusion into the sample, even at the ambient oxygen partial pressure, and thus increases the driving force for densification over conventional sintering, leading to enhanced densification compared to sintering [17].

Since the composition and crystallinity of LLZTO-Al samples sintered in different atmospheres are almost the same, the improvement of conductivity performance mainly stems from material densification with the increase of oxygen partial pressure (P_{O_2}) when sintering. Owing to high temperature sintering, the sintering atmosphere influence on the stoichiometries (e.g. oxygen stoichiometry) and thus the conductivity cannot be ruled out. However from XRD this garnet framework is robust enough even under oxygen-free sintering. The P_{O_2} variation would not induce serious nonstoichiometry, oxygen escape and structure collapse. At high temperature, the oxygen in voids or grain boundaries is prone to diffuse and dissolve into the lattices or oxygen vacancies of oxide ceramics, while nitrogen and argon are difficult to migration through lattices. As a consequence, the pores filled by oxygen gradually shrink and finally disappear, and the pores filled by inert gas are remained during sintering. Therefore, we can clearly observe the tendency that the density and conductivity of LLZTO-Al are improved by tuning the sintering atmospheres from nitrogen, air

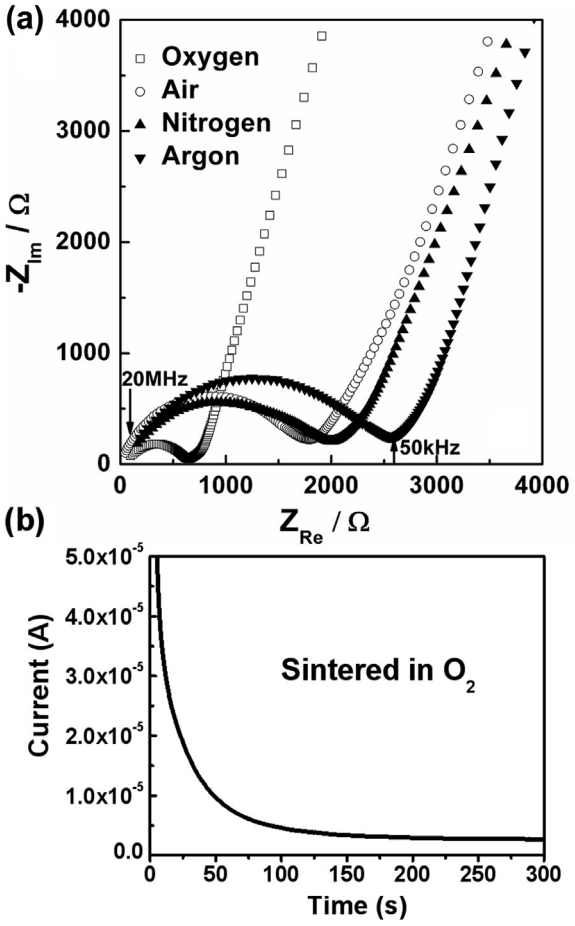

Fig. 3. (a) Impedance spectra measured at 25 °C for LLZTO-Al samples sintered in different atmospheres. (b) Potentiostatic polarization current as a function of measuring time at 25 °C for oxygen sintered sample.

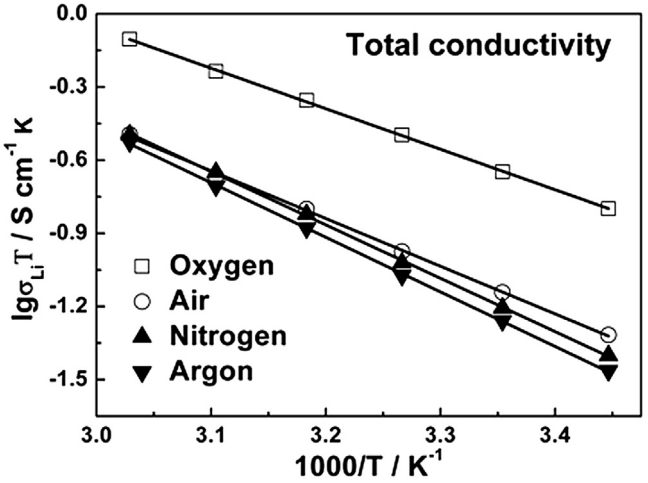

Fig. 4. Arrhenius plots of total conductivities for LLZTO-Al samples undergoing different atmosphere sintering.

(mixture of nitrogen and oxygen) to oxygen. We have not intentionally attempted to mix oxygen with inert gas to adjust an exact P_{O_2}. We predict that a higher P_{O_2} (e.g. 60% and 80% oxygen) than in air (about 20% oxygen) may enhance densification and conductivity to a certain extent, at least comparable to those obtained by air sintering. However, from the present data, the conductivity change as a function of P_{O_2} is likely nonlinear.

4. Conclusions

In summary, cubic garnet ceramic electrolytes of high density (96%) and conductivity (7.4×10^{-4} S cm^{-1}) are obtained by optimizing sintering atmospheres to increase the oxygen partial pressure. Flowing oxygen sintering is found to be most effective to remove the pores near grain boundaries and reduce the negative contribution of grain boundaries on conductivity, and can be extended to other oxide electrolytes. The total conductivity is expected to further improve by optimizing multi-factors, e.g. doping, atmosphere sintering, liquid phase addition and sintering, hot-pressing [27]. In view of the wide electrochemical stability window up to 7 V [22], LLZTO-Al is a promising candidate as solid electrolyte for all-solid-state lithium batteries.

Acknowledgments

The authors would like to thank the project supported by the National Natural Science Foundation of China under Grant No. U1232111. The beamline of BL14B1 in the Shanghai Synchrotron Radiation Facility are acknowledged for the X-ray measurement and data analysis. C. L. Li would like to thank the support from the “Hundred Talents” program of the Chinese Academy of Sciences.

References

[1] P. Knauth, Solid State Ionics 180 (2009) 911–916.
[2] C.L. Li, B. Zhang, Z.W. Fu, Thin Solid Films 515 (2006) 1886–1892.
[3] X.H. Yu, J.B. Bates, G.E. Jellison, F.X. Hart, J. Electrochem. Soc. 144 (1997) 524–532.
[4] C.L. Li, Z.W. Fu, J. Electrochem. Soc. 154 (2007) A784–A791.
[5] Y. Inaguma, L.Q. Chen, M. Itoh, T. Nakamura, Solid State Ionics 70 (1994) 196–202.
[6] G.Y. Adachi, N. Imanaka, H. Aono, Adv. Mater. 8 (1996) 127–135.
[7] R. Kanno, M. Maruyama, J. Electrochem. Soc. 148 (2001) A742–A746.
[8] F. Mizuno, A. Hayashi, K. Tadanaga, M. Tatsumisago, Adv. Mater. 17 (2005) 918–921.
[9] C.L. Li, L. Gu, J. Maier, Adv. Funct. Mater. 22 (2012) 1145–1149.
[10] R. Murugan, V. Thangadurai, W. Weppner, Angew. Chem. Int. Ed. 46 (2007) 7778–7781.
[11] M. Huang, A. Dumon, C.-W. Nan, Electrochem. Commun. 21 (2012) 62–64.
[12] J. Han, J. Zhu, Y. Li, X. Yu, S. Wang, G. Wu, H. Xie, S.C. Vogel, F. Izumi, K. Momma, Y. Kawamura, Y. Huang, J.B. Goodenough, Y. Zhao, Chem. Commun. 48 (2012) 9840–9842.
[13] H. Buschmann, J. Doelle, S. Berendts, A. Kuhn, P. Bottke, M. Wilkening, P. Heitjans, A. Senyshyn, H. Ehrenberg, A. Lotnyk, V. Duppel, L. Kienle, J. Janek, Phys. Chem. Chem. Phys. 13 (2011) 19378–19392.
[14] A. Logeat, T. Koehler, U. Eisele, B. Stiaszny, A. Harzer, M. Tovar, A. Senyshyn, H. Ehrenberg, B. Kozinsky, Solid State Ionics 206 (2012) 33–38.
[15] Y. Kihira, S. Ohta, H. Imagawa, T. Asaoka, ECS Electrochem. Lett. 2 (2013) A56–A59.
[16] J. Wolfenstine, E. Rangasamy, J.L. Allen, J. Sakamoto, J. Power Sources 208 (2012) 193–196.
[17] J.L. Allen, J. Wolfenstine, E. Rangasamy, J. Sakamoto, J. Power Sources 206 (2012) 315–319.
[18] W.E. Tenhaeff, E. Rangasamy, Y.Y. Wang, A.P. Sokolov, J. Wolfenstine, J. Sakamoto, N.J. Dudney, ChemElectroChem (2013), http://dx.doi.org/10.1002/celc.201300022.
[19] P. Sun, C.N. Xu, M. Akiyama, T. Watanabe, J. Am. Ceram. Soc. 82 (1999) 1447–1450.
[20] J.J. Choi, J. Ryu, H.E. Kim, J. Am. Ceram. Soc. 84 (2001) 1465–1469.
[21] Y. Abe, K. Kakegawa, J. Am. Ceram. Soc. 85 (2002) 473–475.
[22] S. Kumazaki, Y. Iriyama, K.-H. Kim, R. Murugan, K. Tanabe, K. Yamamoto, T. Hirayama, Z. Ogumi, Electrochem. Commun. 13 (2011) 509–512.
[23] M. Kotobuki, K. Kanamura, Y. Sato, K. Yamamoto, T. Yoshida, J. Power Sources 199 (2012) 346–349.
[24] A.A. Hubaud, D.J. Schroeder, B. Key, B.J. Ingram, F. Dogan, J.T. Vaughey, J. Mater. Chem. A (2013), http://dx.doi.org/10.1039/c3ta11338h.
[25] S. Narayanan, F. Ramezanipour, V. Thangadurai, J. Phys. Chem. C 116 (2012) 20154–20162.
[26] X.X. Guo, N. Sata, J. Maier, Electrochim. Acta 49 (2004) 1091–1096.
[27] Y.Q. Li, Y. Cao, X.X. Guo, Solid State Ionics 253 (2013) 76–80.